LLNL-TR-401277

LAWRENCE
LIVERMORE
NATIONAL
LABORATORY

Final Report for Plutonium and Quantum Criticality LDRD 03-ERD-077

M. J. Fluss, S. K. McCall, B. W. Chung, G. F. Chapline, D. D. Jackson, R. H. Heffner, R. G. Haire

February 12, 2008

Disclaimer

This document was prepared as an account of work sponsored by an agency of the United States government. Neither the United States government nor Lawrence Livermore National Security, LLC, nor any of their employees makes any warranty, expressed or implied, or assumes any legal liability or responsibility for the accuracy, completeness, or usefulness of any information, apparatus, product, or process disclosed, or represents that its use would not infringe privately owned rights. Reference herein to any specific commercial product, process, or service by trade name, trademark, manufacturer, or otherwise does not necessarily constitute or imply its endorsement, recommendation, or favoring by the United States government or Lawrence Livermore National Security, LLC. The views and opinions of authors expressed herein do not necessarily state or reflect those of the United States government or Lawrence Livermore National Security, LLC, and shall not be used for advertising or product endorsement purposes.

Final Report for
Plutonium and Quantum Criticality
LDRD 03-ERD-077
Jointly funded by
CMS & DNT LDRD Funds

Michael Fluss[1], Scott McCall[1], Brandon Chung[1], George Chapline[1], Damon Jackson[1], Robert Heffner[2], Richard Haire[3]

[1]*Lawrence Livermore National Laboratory, Livermore CA 94550*
[2]*Los Alamos National Laboratory, Los Alamos NM 87545*
[3]*Oak Ridge National Laboratory, Oak Ridge TN 37831*

Abstract:

Plutonium possesses the most complicated phase diagram in the periodic table, driven by the complexities of overlapping 5*f* electron orbitals. Despite the importance of the 5*f* electrons in defining the structure and physical properties, there is no experimental evidence that these electrons localize to form magnetic moments in pure Pu and the $^+\mu$SR measurements included here place an upper limit of $<0.001\mu_B$ for the magnetic moment on Pu.. Instead, a large temperature independent Pauli susceptibility indicates they form narrow conduction bands. Radiation damage from the α−particle decay of Pu creates numerous defects in the crystal structure which produce a significant temperature dependent magnetic susceptibility, $\chi(T)$, in α-Pu, δ-Pu(4.3at%Ga), and $Pu_{1-x}Am_x$ alloys (δ-Pu phase). This effect can be removed by thermal annealing above room temperature. By contrast, below 35K the radiation damage is frozen in place permitting the evolution in $\chi(T)$ with increasing damage to be studied systematically. This leads to a two component model consisting of a Curie-Weiss term and a short-ranged interaction term consistent with disorder induced local moment models. Thus it is shown that self-damage creates localized magnetic moments in previously non-magnetic plutonium. This effect is greatly magnified in some $Pu_{1-x}Am_x$ alloys where an apparent damage-induced phase transition occurs at low temperatures near Stage I annealing which results local moments on the order of 1 μ_B/Pu. The phase is metastable, and anneals away at higher temperatures.

The physical properties of plutonium are controlled by its valence electrons, particularly the 5f electrons and are very sensitive to perturbations. Understanding the nature of these electrons and the influence of radiation damage on their behavior thereby informs our knowledge about the underlying physics of plutonium. This deeper understanding of plutonium metal relates directly to the core competencies of the laboratory. This report is a summary of a number of papers published during the course of this project[1-8] and includes the results of muon spin resonance, magnetic susceptibility, and radiation damage measurements in plutonium and PuAm alloys..

Among the interesting properties of plutonium is a complex phase diagram, which at ambient pressure exhibits six
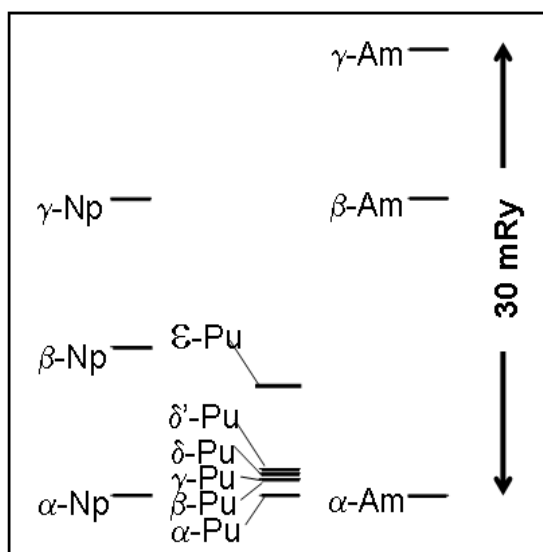
Fig. 1 Relative energy scales for different phases of Np, Pu, and Am. The five lowest energy phases of Pu are separated by less than 2 mRyd.

distinct solid-state phases below the melting temperature. These phases are narrowly spaced in energy, with the five lowest energy phases separated by less than 2 mRyd, placing them on a molecular energy scale as compared to the more typical 10-20 mRyd scale typical of metals such as neighboring Np and Am[9] as shown schematically in Fig. 1. While there is no theoretical consensus as to the origin of the low density fcc δ-phase of Pu[9-15] there is an understanding that the organization of the spin and orbital moments play a key role in stabilizing this phase. The lack of significant magnetic moments is a central issue among theorists, and inspired a recent experimental review[16] painstakingly describing the evidence against the existence of magnetic moments in plutonium. Recent μSR^{+} studies for α- and δ-phase Pu further support this absence of magnetic moments, placing the upper bound on frozen moments at 0.001 μ_B[4]. However, all solid Pu phases possess large magnetic susceptibilities suggesting they border on becoming magnetic. Consistent with this observation

and general predictions of narrow 5*f* bands in plutonium, are large electronic contributions to the specific heat in both α-Pu and alloy-stabilized δ-Pu, qualifying each as a highly correlated electron system[17].

Often, local magnetic moments can be induced in nearly magnetic systems by imposing a suitable perturbation. One such method is to increase disorder by introducing a low concentration of impurities via chemical substitution. For example, when very dilute quantities of Fe, Co, or Ni are doped into non-magnetic Pd they induce remarkably large magnetic moments by polarizing the surrounding lattice[18, 19]. Similarly, one-half atomic percent Pu doped into La depresses the superconducting T_c= 5.9K by nearly 2K, effectively acting like a magnetic impurity, while actinides such as U and Am reduce T_c by only 0.2K[20]. Surprisingly, the converse experiment: doping non-magnetic impurities such as Zn or Li into the antiferromagnetic Cu-O planes of the high temperature superconducting cuprates (HTSC) also induces significant local moments (as large as $1\mu_B$ per impurity) on the neighboring Cu atoms[21, 22]. Similarly, magnetic moments arise from point defects (vacancies in the copper-oxide planes) produced by electron irradiation of HTSCs, where the irradiation permits a systematic study of samples as a function of defect concentration (damage)[23]. Plutonium-239, with a half-life of 24,110 years, radioactively decays by emission of a 5.04 MeV α-particle and corresponding 85.8 keV U recoil, which produce numerous defects in the underlying lattice. These defects primarily consist of vacancies (unoccupied lattice sites) and interstitials (displaced atoms that come to rest in a location between the normal lattice sites). The resulting self-damage increases the magnetic susceptibility in a manner indicative of local moments which would

not be all that surprising were the underlying plutonium magnetic. That these moments develop in a non-magnetic system is quite remarkable and implies this perturbation provides an observational window into the heretofore hidden nature of the 5f electrons, effectively driving them toward a more localized state.

One advantage of exploiting the radiation damage from nuclear decay is that by measuring the magnetic properties as a function of time it permits continuous observation of how the influence of damage evolves. However, the defects produced by the radioactive decay of ^{239}Pu are more complex than the isolated vacancy and interstitial pairs (Frenkel pairs) created by an electron or proton beam. Molecular dynamics models indicate that the decay α-particle travels ~10 μm in δ-Pu losing most of its energy by scattering from electrons, but near the end of its range (the last 0.8 μm), it begins to ballistically scatter with atoms producing ~265 vacancy and interstitial pairs. By contrast, the U recoil travels only ~0.012 μm initiating a dense displacement cascade of ~2300 vacancies and interstitials, roughly 70% of which are estimated to recombine[24] during the following tens of picoseconds as the lattice rapidly cools. Previous work[25-28] examined changes in resistivity and volume due to self damage in plutonium. Recently, the temperature dependence of the resistivity of vacancies and vacancy clusters Pu(Ga) was shown to exhibit a -*ln*(T) behavior, suggesting a defect-induced Kondo-like behavior[29], analogous to that seen in hole doped superconductors subjected to electron irradiation[23]. Here we report the discovery and characterization of time and temperature dependent magnetic susceptibility caused by accumulating damage in α-Pu and δ-Pu(4.3 at.%Ga) (hereafter denoted δ-Pu) which is fully reversible by thermal annealing.

Experimental Details

Two specimens were prepared from an aliquot of Pu, which had been electro-refined two years prior to the experiments: α-Pu (99.98% pure), and δ-Pu (4.3 at.%Ga). For the μSR experiments, samples were formed into 12 mm diameter and 0.1 mm thick disks, which were encapsulated in Kapton and sealed under helium inside a titanium cell with Ti-foil beam windows. These experiments were performed at the M20 surface muon channel at TRIUMF in Vancouver, Canada. For the magnetization experiments, each sample was machined into 1x2x2 mm bars, and then mechanically and chemically cleaned of oxide, yielding specimens of 56.8 mg and 45.4 mg respectively. The isotopics for both specimens were similar, having been determined by inductively coupled plasma mass spectroscopy: ^{239}Pu (93.7%), ^{240}Pu (5.86%), and ^{238}Pu (0.17%), while the magnetic impurities in atomic ppm were; Fe (231), Ni (24), Cr (12) and Mn (10). $Pu_{1-x}Am_x$ (0.18<x<0.29) alloys were synthesized at Oak Ridge National Laboratory using the same Pu starting material, and ^{243}Am, with sample masses of ~15-70 mg depending on the Am concentration. Specimens were coated with ~5 μm polyimid to contain radioactive spall, sealed under helium in a 20 cm long cartridge-brass tube and measured in a SQUID magnetometer (Quantum Design MPMS-5). All measurements were made in a constant applied magnetic field of 3T, for which the background contribution due to the tube was <1%, and as most results reported here are differential measurements (*i.e.* changes in signal as a function of time), it self cancels. The high thermal conductivity of the tube acts as a heat sink for the sample and ensures thermal stability. The maximum self-heating effect was measured as ~0.05K at 2K. Repeated

measurements at each temperature showed no trend indicative of a thermal lag between the system thermometer and the sample. Extensive isothermal measurements as a function of applied magnetic field were also conducted.

Plutonium Results

Muon spin resonance measurements, shown in Fig. 2 permit the setting of an upper limit on the ordered moment, μ_{ord} in both α–Pu and δ-Pu specimens. Using a typical muon hyperfine field found in f-electron systems of $H_{hyp} \sim 0.1$ T/μ_B and taking $\Delta \sim 0.05$ μs^{-1} as an upper limit for the relaxation rate from the hypothesized ordering, one has $\mu_{ord} \leq \gamma_\mu/(H_{hyp}\Delta) \sim 10^{-3}\mu_B$ at T = 4K. If there is a sizeable localized component to the f-electron density in δ-Pu, why might it be unobservable? It is possible
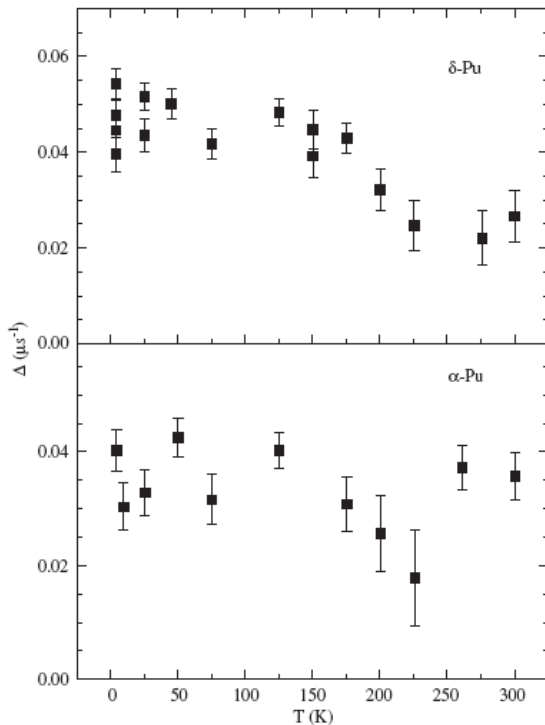

Fig. 2 ZF static Gaussian Kubo-Toyabe widths in α- and δ-Pu between T = 3.8 – 300K. Muon diffusion may cause the reduction of the linewidth above 200K in δ-Pu.

that the spins do not order until T << 4K, so that the mean fluctuation rate is still too rapid to produce a significant relaxation rate $1/T_1$ in the time scale of our measurement. An estimate of the lower limit for τ^{-1} can be obtained by taking:

$$1/T^{-1} = 2(\gamma_\mu H_{hyp})^2\tau << \Delta(4K).$$

Then $\tau^{-1} >> 3.6 \times 10^{11}$ s^{-1}, corresponding to an upper limit for the f-electron linewidth Γ = 0.24 meV, again for $H_{hyp}\sim 0.1$ T/μ_B. This is a few times lower than the Γ estimated from NMR measurements in Pu(Ga 1.5%)[30].

The magnetic susceptibility, defined as $\chi(T)$=M/H, of freshly annealed (350K for 1 hour) α–Pu and δ-Pu specimens measured between 2K<T<350K is shown in Fig. 3. By noting the scale of Fig. 3 it is evident that the dominant contribution to $\chi(T)$ in both specimens is the temperature independent Pauli susceptibility, which is particularly clear in the case of α–Pu, where $\chi(T>100)$ = 511±1 μemu/mol, consistent with other reported values[30]. Lower temperatures reveal a Curie impurity tail contributing less than 5% to the overall signal, dominated by the 231 ppm Fe impurities present in the samples as a result of the manufacturing process. The temperature dependence of the data below 40K fit a Curie-Weiss law: $\chi(T) = C/(T-\theta)$ where C, the Curie constant, is proportional to the square of the effective moment and θ, the paramagnetic Weiss temperature, provides a measure of the exchange energy. Such a fit results in an effective magnetic moment of 4.16μ_B/Fe, somewhat less than the 5.92 μ_B/Fe (4.90μ_B/Fe) expected were all the Fe impurities effectively trivalent(divalent) with S=5/2 (3/2), but not unreasonable as some fraction of the Fe has likely been subsumed into intermetallic Pu$_6$Fe[31].

The $\chi(T)$ for δ-Pu is more complex, though still dominated by a Pauli term, with the

magnetic susceptibility increasing less than 10% when cooled from 350K and 2K. There are several features in the $\chi(T)$ plot— a low temperature Curie tail due to the same impurities observed in the α–Pu sample, and a small peak at ~33K, likely due to second phases of $PuGa_3$ and $PuGa_2$ at the level of a few hundred ppm[32, 33]. If these second phases rise to a concentration of order 0.1%, which could result from incomplete homogenization of the Ga, they would fully account for the gentle slope observed for T>40K. This slope is also consistent with previous observations of Ga stabilized δ-Pu[34] which did not extend to sufficiently low temperatures to rule out second phases. Isothermal magnetization measurements to 5.5T at 5K on both specimens after annealing at 350K for 1hr are strongly linear, and thus support the interpretation of the Pauli term as the dominant contribution.

The magnetic susceptibility increases as a function of time, initially at the rate of several hundred ppm/hr at 5K for both specimens. When the specimen is maintained at low temperatures, the magnetic susceptibility continues to increase so that after a month the lowest temperature values have increased more than ten percent above the magnetic susceptibility of the originally annealed specimen, as illustrated in the inset of Fig. 3. Here $\chi(T < 30$ K$)$ is plotted for specimens aged 42 days at T $\leq$ 30K along with the data of freshly annealed samples, demonstrating the strong temperature dependence that develops as the sample accumulates damage at low temperatures.

Any study of radiation damage must carefully assess the relationship between the radioactively generated damage cascades, and thermally activated annealing which tends to alter and eventually remove damage. There are two important temperatures to identify: the temperature
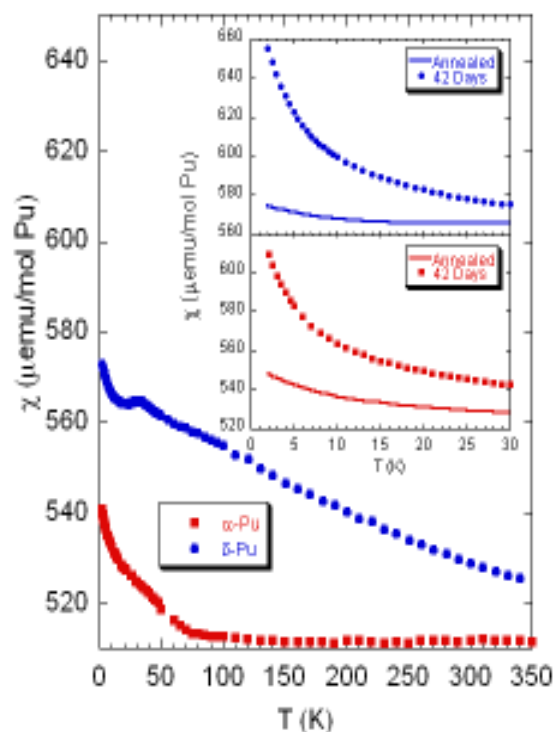

Fig. 3 $\chi(T)$ for annealed α-Pu and stabilized δ-Pu(4.3at%Ga). The Curie tail in α-Pu is consistent with ~200 ppm Fe impurities, while the gentle slope in δ-Pu may arise from small quantities of $PuGa_x$ ($2 \leq x \leq 3$) second phases. The inset shows the low temperature $\chi(T)$ for annealed and aged (42 days below 30K) specimens.

where significant annealing commences; and the temperature at which the damage is completely annealed away apart from the radio-decay products, predominately U and He. Finally, some assessment of which point defects are most responsible for changes in the magnetic properties should be considered.

In the present work, damage is accumulated for several weeks at 5K, after which the specimen is soaked for a fixed time (isochronal) at successively higher annealing temperatures (T_{An}), with each anneal followed by a measurement at 5K. From this data the resulting fraction of the excess magnetic susceptibility retained after each anneal, *i.e.*

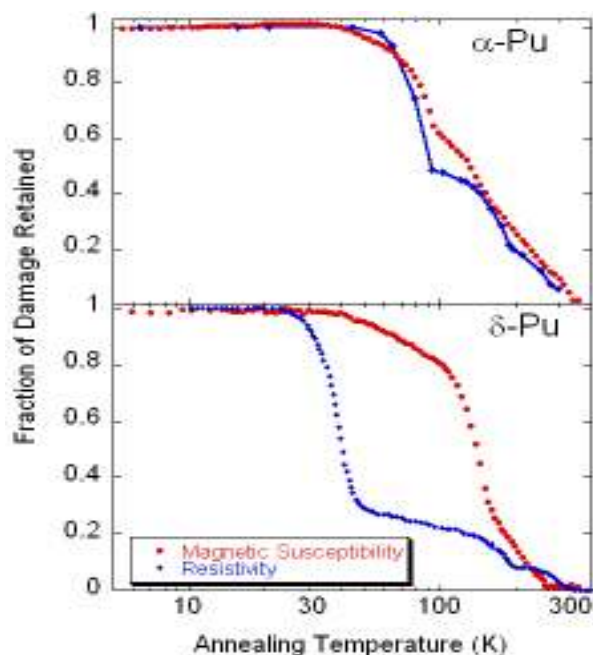$$f_\chi = [\chi(5K)|_{T_{An}} - \chi(5K)|_{T_{350K}}] \qquad (1)$$

Fig. 4 Isochronal annealing curves for α-Pu and Ga stabilized δ-Pu illustrating that damage is frozen in place below ~30K. The red circles are the magnetic susceptibility measurements from this work while the blue diamonds are resistivity data taken from references [25] and [29] respectively.

can be extracted. The f_χ data is then normalized and plotted (red circles) as a function of T_{An} in Fig. 4 for both specimens. For comparison, Fig. 4 includes data from previously reported experiments[25, 35] which used resistance to study the annealing of accumulated damage (blue diamonds) on specimens with similar but not identical annealing protocols or compositions. It is noteworthy, that the δ-Pu resistive annealing curve was obtained on a specimen with a different Ga concentration (3.3 at% Ga) and after a significantly shorter damage accumulation period (3 days) than the other data reported here. All four measurements consistently show a flat region below 30K, indicating little or no annealing takes place up to this temperature—the defects are frozen in place. Above this temperature the onset of

annealing is indicated by the decrease in signal magnitude with signs of specific stages related to the activation energies for interstitials, vacancies, and their aggregates. Finally, the data provide an estimate of the temperature for complete annealing where vacancy clusters dissolve and the specimens are "reset" to an undamaged condition. This occurs at ~315 K for α-Pu and ~300 K for δ-Pu. Of course, decay products (U and He) accumulate and cannot be removed by this procedure, but their contribution to the overall magnetic susceptibility is below the threshold of detection in these experiments. By remaining at T<30K, the samples dope themselves with damage cascades proportional to time and can be effectively returned to a zero time state by annealing above room temperature.

On the whole, the magnetic susceptibility annealing shows evidence for distinct annealing stages similar to the resistive annealing, but a comparison of the two techniques provides additional insight. The situation for the α-Pu is qualitatively similar in annealing behavior over the entire temperature range of the annealing study for both techniques. However for the δ-Pu it appears that the large drop observed in the resistive annealing above 30 K is missing from the magnetic susceptibility annealing curve. This annealing stage is believed to be where interstitials begin to move and annihilate with nearby vacancies or become trapped near other local defects such as impurities. Instead, the most dramatic reduction in the magnetic susceptibility annealing curve is "deferred" until well above 100 K, which based on the resistive annealing curve approaches stages usually associated with vacancy interactions. These results suggest that interstitials do not contribute as significantly to the excess magnetic susceptibility in the δ-phase as do the vacancies, an idea which is reasonable considering the fcc delta phase(15.92 g/cm^3)

is significantly less dense than the monoclinic alpha phase(19.84 g/cm^3). The idea that "spinless" vacancies may induce magnetic moments on the surrounding lattice is also consistent with the conclusions drawn from radiation damage and doping studies of HTSC compounds[23].

For each sample, the magnetic susceptibility was measured as the temperature was repeatedly cycled from 2-30K for a period exceeding 40 days. Fig. 5 illustrates the time (damage) dependence of the magnetic susceptibility for several representative isotherms. The points are actual data, and the lines are best fits to the following equation:

$$\chi(t,T) = \chi_i(T) + \chi_v(T)(1 - e^{-t/\tau}) + \chi'_D(T)t \quad (2)$$

where $\chi_i(T)$ is the initial magnetic susceptibility of the annealed specimen. The later two terms describe the excess magnetic susceptibility arising from the self-damage and therefore explicitly depend on time and are zero when t=0. The different time dependences reflect two distinct contributions, where the coefficients, $\chi_v(T)$, and $\chi'_D(T)$, are free parameters for each isotherm with no assumed T dependence. The prime on the coefficient in the third term, $\chi'_D(T)$, emphasizes that the contribution to the magnetic susceptibility from this term is per unit time, *i.e.* μemu/mol/day. Attempts to fit other probable models, such as a stretched exponential, led to coefficients that fluctuate strongly with temperature and thus fail to provide a self consistent description of the data.

Discussion

Phenomenologically, the damage cascade generated by each α-decay may be considered to increase the magnetic susceptibility within an effective volume, δV of arbitrary shape and not necessarily simply connected. This effective volume must be at least as large as the damaged region, although there is no *a priori* reason it cannot be significantly larger, provided δV<<V, the sample volume. Thus, the overall fraction of the sample magnetically influenced by the first decay is given by δV/V. Assuming the susceptibility within δV is not further altered by subsequent and overlapping δVs, the expected volume fraction damaged by the second α-decay is just (δV/V)(1-δV/V), where the second term is the fraction of the sample uninfluenced by the previous event. Similarly, for the nth event, the expected volume fraction influenced is:
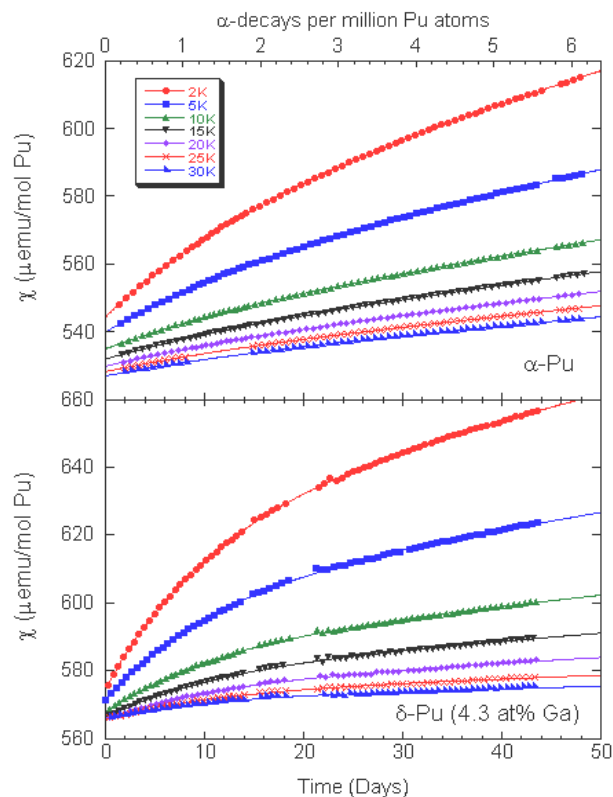

Fig. 5: Representative isothermal magnetic susceptibilities for α-Pu and δ-Pu (4.3at%Ga) plotted as a function of time (number of α-decays). The lines are fits to Eq. (2) described in the text.

$$\lim_{n \to \infty} \frac{\delta V}{V}\left(1 - \frac{\delta V}{V}\right)^{n-1} = \frac{\delta V}{V}\,exp\left(-n\frac{\delta V}{V}\right) \qquad (3)$$

The total volume fraction of the sample magnetically influenced by damage after n events is simply the sum over all the individual volumes, which after integration is $(1 - exp[-n(\delta V/V)])$. Recasting this as a function of time, $t = n/\lambda$, where λ is the α-decay rate of the specimen, and defining a characteristic time, τ, as: $1/\tau = (\delta V/V)\lambda$, then Eq. (3) becomes: $(1-e^{-t/\tau})$. This is simply the time dependence of the $\chi_v(T)$ term described in Eq. (2).

The 32 α-Pu isotherms are all described by a single characteristic time: $\tau_\alpha = 15.8 \pm 0.5$ days, while $\tau_\delta = 11.2 \pm 0.3$ days describes all 37 δ-Pu isotherms, subsets of which are plotted in Fig 4. Converting these characteristic times to effective volumes per cascade yields 9900 nm^3 (~500,000 atoms) for α-Pu and 13,600nm^3 (~550,000 atoms) in the case of δ-Pu. Both quantities agree within 10% in terms of atoms influenced, despite the 40% longer characteristic time for the α-Pu sample. To put these numbers in context, consider that a recoiling U atom travels 12 nm in δ-Pu, which if treated as the diameter of a sphere encapsulating the recoil cascade, equates to 35,000 atoms—an order of magnitude smaller than suggested by Eq. (2). Of course, the origin of the larger effective volume may just reflect extended features such as strain fields or longer ranged magnetic interactions not evident from molecular dynamics calculations.

The fits of the data to Eq. (2) result in a systematic and monotonic temperature dependencies of the coefficients, $\chi_v(T)$ and $\chi'_D(T)$, as illustrated in Fig. 6. The contribution from $\chi_v(T)$ is shown in Fig. 6(a), while the inset shows the inverse magnetic susceptibility as a function of temperature demonstrating that it fits well to a Curie-Weiss law: $\chi(T) = C/(T-\theta)$. The fit requires no temperature independent term (i.e. χ_0 in a modified Curie-Weiss fit), either positive or negative in value, indicating there is no appreciable change in Pauli susceptibility due to the damage. Therefore, the conduction bands are not appreciably altered within the bubble regions. The Curie constant, C, obtained from the fit is 128 μemu/mol·K for α-Pu (248 μemu/mol·K for δ-Pu), equivalent to an average effective moment of 24.6μ_B per α-particle decay in α-Pu (33.4μ_B per α-particle decay in δ-Pu), or using the number of atom estimates obtained above, an average moment of 0.033μ_B per α-Pu (0.045μ_B per δ-Pu).

This average moment is most probably concentrated in discrete clusters with larger magnetic moments scattered throughout the
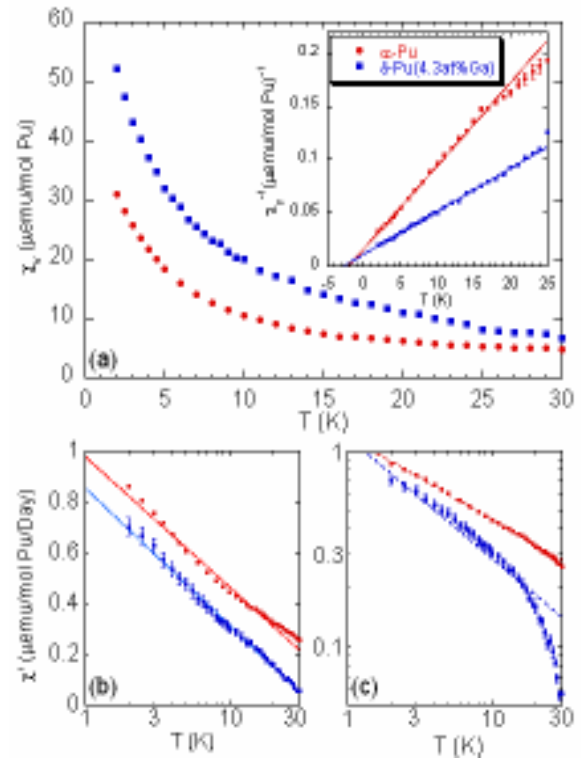

Fig. 6 Temperature dependence of self-damage contributions. (a) the contribution from χ_v with the inset illustrating a Curie-Weiss fit. (b) χ'_D as semi-log plot emphasizing -ln(T) dependence (solid lines) and (c) as a log-log plot showing power law fits (dashed lines).

effective volume instead of a uniform moment evenly spread throughout the volume. In analogy with the defect induced moments of the HTSCs, the cluster of Pu atoms surrounding a vacancy would possess a moment due to increased localization of the 5f electrons. The Curie-Weiss behavior observed in both the electron irradiated and non-magnetic Zn doped HTSCs is attributed to Kondo-like behavior of the Cu ions surrounding the impurity. Kondo systems have Curie-Weiss behavior at high temperatures and then below a characteristic energy scale set by T_K (the Kondo temperature), the conduction electrons antiferromagnetically couple with the local moments to form a non-magnetic ground state. Typically the Kondo temperature is about a quarter of the paramagnetic Weiss temperature, which is $\theta_P = -2.0$ K for α-Pu (-2.8 K for δ-Pu) with the negative sign indicating antiferromagnetic correlations. So if damage is inducing Kondo behavior, T_K is less than 1 K and Curie-Weiss behavior is expected in the experimentally measured temperature range, while the comparable magnitude of θ_P for both allotropes implies little sensitivity to the details of the local crystal structure. This picture is consistent with the isochronal annealing data of δ-Pu, which show that the damage induced magnetic susceptibility changes most rapidly when the vacancies become mobile. Of course, a Pu vacancy in the fcc δ-phase has 12 nearest neighbors and the monoclinic α-phase has a comparable number[36] while there are only four relevant nearest neighbors in the planar HTSCs, so each vacancy should influence more atoms in Pu. Furthermore, the self-damage cascades in Pu are more complicated than the isolated vacancies or Zn atoms of the HTSC materials.

These more complicated damage cascades may explain the $\chi'_D(T)t$ term. While linear in time, it likely represents the leading term

of an exponential with a much longer characteristic time and thus a correspondingly smaller effective volume thereby remaining in the dilute limit. Taken as short-ranged interactions, they will contribute appreciably only when multiple defects are in close proximity, such as are expected within the cascade resulting from the U recoil. Similarly, such dense concentrations of defects may be a second-order effect that begins to grow in regions of overlapping damage where the defect density surpasses a critical threshold. Fig. 4(b) shows the temperature dependence of this term plotted on a semilog scale to emphasizes the fit of $\chi'_D(T) \propto -ln(T)$ and that α-Pu and δ-Pu have remarkably similar slopes of -0.224 μemu/mol-Pu/Day and -0.236 μemu/mol-Pu/Day respectively. This $-ln(T)$ behavior is described by the Kondo disorder model, initially proposed by Bernal et al[37] to explain $UCu_{5-x}Pd_x$ and later expanded theoretically by Miranda et al[38, 39]. Unlike the standard Kondo model, which assumes a dilute concentration of localized spins, here disorder creates a broad distribution of low-T_K values which lead to a logarithmic temperature dependence in the magnetic susceptibility and non-Fermi liquid behavior. The implication is that T_K depends on the local density of defects, and the inherently random nature of the self-damage will naturally lead to a distribution of defect densities. Since the T_K depend on damage induced disorder, the local symmetry of undamaged regions is not relevant which is reflected in the consistent slopes for both allotropes.

A second model, also developed to describe $UCu_{5-x}Pd_x$, has been presented by Castro-Neto and coworkers[40, 41] where disorder drives a competition between the Kondo effect and the Ruderman-Kittel-Kasuya-Yosida (RKKY) interaction. In the RKKY interaction, the conduction electrons couple local moments together, either

ferromagnetically or antiferromagnetically depending on the distance between the moments. This model postulates a Griffiths phase[42], wherein clusters of local moments are magnetically coupled within a non magnetic background. Here, when defect induced local moments are sufficiently close, they begin to couple together magnetically, leading to $\chi(T) \sim T^{-1+\lambda}$ and a prediction of non-Fermi liquid behavior. Over limited temperature ranges, a weak power law proportional to $T^{-1+\lambda}$ with $\lambda \approx 1$ can be difficult to distinguish from logarithmic behavior. The lines of Fig. 6(c) show the result of least squares fits to the data with $\lambda = 0.57$ (0.38) for α-Pu (δ-Pu). The fit is improved as compared to the $-ln(T)$ fit for α-Pu but markedly worse in δ-Pu, so there is a clear distinction between the two allotropes in this interpretation.

It is worthwhile to make note of the relative magnitudes of the two time dependant contributions: the $\chi'_D(T)$ term is larger for α-Pu than for δ-Pu in contrast to the $\chi_v(T)$ term, where the δ-Pu contribution is larger. A relative contribution also shows that $\chi'_D(T)t \approx \chi_v(T)$ after 25 days for α-Pu, but takes nearly 70 days for δ-Pu. Since the Castro-Neto model is built on a competition between the RKKY and Kondo energies, one possible explanation is that the RKKY interaction strength is so much weaker in δ-Pu as to not have significant influence. This is not an unreasonable assertion. Normally the RKKY interaction is long ranged, but disorder weakens the interaction strength, making it decay exponentially with distance and thus become effectively short-ranged[40, 43]. If the average distance between magnetically interacting defects for both α-Pu and δ-Pu is the same in units of atomic separations, then as δ-Pu is roughly 20% less dense, this will correspond to a larger absolute distance and weaker coupling strength. Additionally, one of

every 25 atoms in δ-Pu is a non-magnetic Ga, further decreasing the RKKY interaction strength, while simultaneously increasing the disorder inherent to the δ-Pu phase. Supplementary studies looking at the influence, if any, of Ga concentration will help clarify this issue.

These radiation damage induced changes in the magnetic susceptibility suggest increased *f*-electron localization and consequentially, reduced metallic bonding. It would not be surprising to see similar changes in other thermodynamic properties such as heat capacity and the lattice stiffness. Indeed, just such an effect has been reported by Migliori where a measurable lattice softening as a function of time (over ~50 hrs.) is observed between 50 and 150K in δ-Pu(2.36 at %Ga)[44].

PuAm alloys

Fig. 7 shows the magnetic isochronal annealing results for δ-Pu$_{1-x}$Am$_x$ (x = 0.224) where the damage was accumulated at sufficiently low temperatures that once formed, the damage cascades are frozen in place. Previous work on radiation damage in PuAm alloys has also investigated the consequence of damage on magnetic susceptibility, but such damage was accumulated near room temperature[45, 46] which as may be observed in Fig. 7, is very close to the annealing stage where small vacancy clusters are unstable. Therefore, measurements of damage accumulated for extended periods of time at room temperature cannot be easily related to the data from this study. There are no resistivity annealing measurements for this or a similar alloy specimen with which to compare, so this data is shown along with the earlier δ-Pu$_{1-x}$Ga$_x$ (x = 0.043) curve for comparison. There are several general similarities, including no observable decrease in the excess magnetic susceptibility (EMS) for

annealing temperatures below 33K, and the return to an effectively fully annealed state just above 300K. However, δ-$Pu_{1-x}Am_x$ (x = 0.224) shows no obvious intermediate states between 60K and 300K, instead just a broad monotonic decrease in the fraction of EMS signal retained. An examination of the derivative suggests there are changes of slope around 100K and around 260K which, from analogy with the δ specimen would be the onset of Stage III and Stage V annealing respectively. These are slightly lower in temperature than observed for delta, but that is not surprising considering the interatomic spacing for the δ-$Pu_{1-x}Am_x$ (x = 0.224) is greater, which should facilitate the mobility of defects. The truly spectacular feature observed in this system is shown in the inset of Fig. 6 where between 35K and 56K the signal from the EMS unexpectedly grows by nearly a factor of 40 before returning to "normal" behavior. This clearly does not indicate that the amount of damage suddenly increases by a factor of 40, but indicates that something very dramatic happens to the
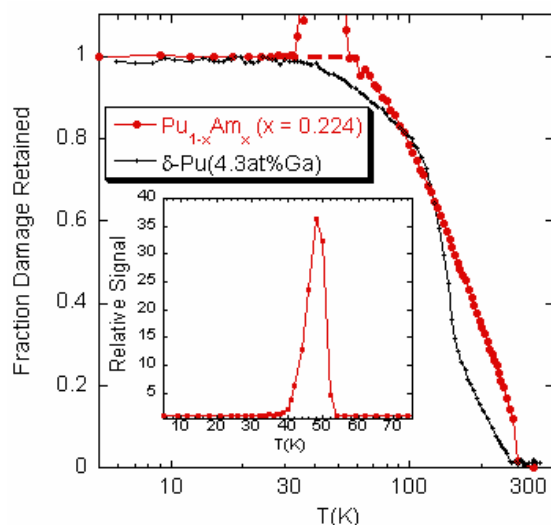

Fig. 7 Isochronal annealing curve for Pu1-xAmx (x=0.224) specimen aged 40 days. The black line shows the stabilized δ-Pu (4.3at%Ga) specimen as a comparison. The inset shows the anomalous increase in signal relative to χ(T=5K) before the onset of annealing.

magnetic susceptibility in the initial stages of annealing, most likely a result of a structural feature which develops during the annealing protocol. Hence, the inset shows this phenomena, plotted in units of emu/mol Pu, as well as relative signal strength where unity is the value of χ(T=5K) when the annealing protocol begins.

More detailed time and temperature studies to investigate this transient feature of the annealing protocol were undertaken. After annealing at 350K for 1 hour, the specimen was again held at low temperatures for 40 days (~6.26 α-decays per million atoms), and then the magnetic susceptibility was systematically measured as it was warmed to and cooled from progressively higher temperatures between 35K and 60K in 5K steps. Measurements were made during both the warming and cooling cycles in 1 K steps with 10 sets of measurements taken over the course of 5 minutes at each temperature. A subset of these measurements is shown in Fig. 8. Fig. 8(a) shows χ(T) on the initial warming to 35K (green circles) after having been maintained at T$\leq$30K for 40 days, during which χ(T=2K) grew from 850 μemu/mol to 1000 μemu/mol. At temperatures above 33K, the magnetic susceptibility begins to increase with temperature. The data showing warming to 45K (red squares) after previously warming to 40K reveal an increase in χ(T=2K) of ~100 μemu/mol, nearly the equivalent to a month of damage accumulation in only a few hours. This shows that warming to temperatures where the first signs of annealing are expected leads to an increase in magnetic susceptibility that remains when cooling to low temperatures again More dramatically, as the temperature increases through 40K, there is a rapid increase in the magnetic susceptibility, which is changing dramatically over the course of minutes as may be observed from the spread of data

points at each temperature. Upon cooling from 45K (blue triangles), the magnetic susceptibility is irreversible, following a different path, resulting in $\chi(T=2K)$ increased by 850 μemu/mol from the data prior to heating. Several other features are noteworthy in the cooling data, including a shoulder at about 30K not observed in the warming data. As the temperature decreases to below 30K, the spread of the isothermal data points shrinks to a negligible value, demonstrating that the defects again become frozen into place and active annealing ceases. This strong time dependence at T > 33K explains why the low temperature $\chi(T)$ values are smaller than the factor of 20 observed for the 45K isochronal anneal (see inset of Fig. 7).

A tremendous increase in magnetic susceptibility is spectacularly demonstrated in Fig. 8(b), where further cycles in temperature extending to 50 and 55K are shown with $\chi(T=2K)$ = 22,500 μemu/mol after the 50K anneal—an increase of 22X over the value obtained after aging at low temperature. A comparison between Fig.8(a) and 8(b) shows a shoulder in the cooling data at both 45K (8a blue triangles) and 50K (8b blue triangles) which is not observed in the warming data. Presently there is no simple explanation for this, but it may be related to relaxation of structures formed at higher temperatures which are not accessible on subsequent heating cycles. Below this shoulder, the damage retained appears to be frozen in place once more as the time dependence of the isothermal magnetic susceptibility becomes constant (within experimental uncertainty). However, in this frozen state there is a remarkable change in the thermodynamic state of the alloy when compared to the state prior to warming. Annealing to 58K rapidly dissipates the observed enhancement and by 60K the anomalously large magnetic susceptibility has vanished both at the
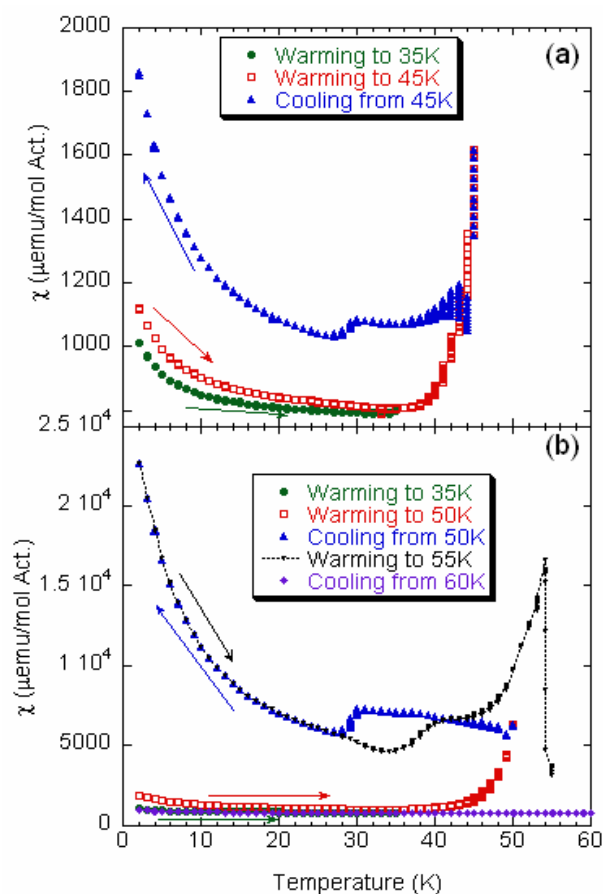

Fig. 8 The magnetic susceptibility increases dramatically and dynamically when warmed after soaking at T<30K for a month. (a) Green curve shows χ (T) warming to 35K, the red curve is systematically warming to 45K after annealing briefly at 40K, and the blue curve shows χ (T) as the sample is cooled back from 45K. (b) Green curve again shows 35K data, while the red (blue) curve shows systematic warming to (cooling from) 50K, and the black curve warming again to 55K. After warming to 50K, χ (T=2K) exceeds its initial value by more than 20X (see text for detailed discussion). Finally, the cooling from 60K data shows a return to the behavior expected for a typical annealing process.

anneal temperature and all temperatures below, as shown by the data cooled from 60K in Fig 8b (purple diamonds) where the extraordinary increase in the magnetic susceptibility has disappeared. On subsequent annealing at higher temperatures the isochronal annealing behavior is now similar to Ga-stabilized δ-Pu.

The low temperature behavior of this large transient excess magnetic susceptibility after annealing to 50K (Fig 8b blue triangles, black triangles) can be fit to a modified Curie Weiss law: $\chi(T) = \chi_0 + C/(T-\theta)$ for $T < 25K$ which results in an enhanced temperature independent contribution of $\chi_0 = 1400$ μemu/mol as compared to an annealed value of ~700 μemu/mol, a paramagnetic Weiss temperature (θ) of -3.9K, and most astoundingly, an effective moment (μ_{eff}) in excess of 1.1 μ_B/Pu atom. Such a dramatic change in a thermodynamic property, from essentially non-magnetic to possessing an effective moment comparable to that of magnetically ordered Pu compounds, such as PuH_2, implies a phase change in this alloy driven by the accumulated damage. This is further supported by the near doubling of χ_0, which implies a dramatic change in the electronic band structure, with this transient phase possessing a much narrower density of states.

The idea that radiation damage could drive a magnetic phase transition in a Pu-Am alloy is worthy of consideration. Pure Pu possesses multiple solid-state phases below the melting temperature, with the α, β, γ, δ, and δ' phases all separated by less than 2 mRyd in energy[9], as compared to the 10-30 mRyd differences in energy between the solid-state phases of the neighboring actinides: Np and Am. Thus, multiple phases of Pu are nearly degenerate, and can be stabilized by perturbations, such as doping with Ga or Am to stabilize the δ-phase. The δ-$Pu_{1-x}Am_x$ (x = 0.224) alloy may also have other nearly degenerate phases, some of which have very different magnetic properties and become accessible by perturbing the system with disorder.

There is insufficient data to form a complete picture of the phenomena observed in this alloy, but one possible interpretation is outlined as follows. As in the other Pu samples discussed in this work, self-damage is frozen in place at low temperature, while simultaneously increasing the entropy of the system. This increase must change the overall free energy of the system, and may lower the free energy of a competing phase below that of the undamaged phase; yet a phase transition is kinetically inhibited at the low temperatures. By warming the system to a point where annealing begins, the barrier is lowered sufficiently for the phase transition to occur, which is reflected as a change in the magnetic (thermodynamic) properties. As the system is further annealed, the new phase grows, as indicated by the further increase in magnetic properties. However, the annealing also reduces the entropy of the system making the new phase less stable, so after sufficient annealing transpires, the original non-magnetic phase again becomes favorable and the alloy reverts to its initial state. Such a phase transition need not consume the entire sample. For example, early stage annealing could nucleate a quantum Griffiths phase in the alloy, where the disorder creates magnetic droplets distributed throughout a paramagnetic background[40, 42]. These droplets might arise at the damage cascades generated by the recoiling nucleus from the α-particle decay where the defect population, and therefore disorder is considerably greater. Additional measurements, particularly specific heat and isothermal magnetization, need to be performed on this alloy to understand the remarkable changes observed in the magnetic susceptibility measurements. Nonetheless, this remarkable, if transient, increase in the magnetic susceptibility may be a sign of new magnetic phases in Pu-Am alloys, and perhaps signal proximity to a stable magnetic phase for the proper combination of Am-doping, disorder, and magnetic field.

Conclusions

Perhaps the most remarkable conclusion drawn from these magnetic measurements is that the radiation damage induces clear evidence of localized magnetic moments in a system where none are observed in the pure state. Elemental α-Pu and Ga stabilized δ-Pu as well as δ-phase PuAm alloys have large Pauli susceptibilities indicative of narrow bands at the Fermi surface. A temperature dependant magnetic susceptibility arises from self-damage at low temperatures without measurably distorting these conduction bands. Isochronal annealing experiments confirm that these increases are due to accumulating radiation damage and may be removed by thermal annealing. Analysis of the time dependence of the damage induced magnetic susceptibility leads to two distinct terms, with differing temperature dependencies. The dominant term at early times may be ascribed to a volume considerably larger than expected from models of the damage cascade alone, which fits well to a Curie-Weiss law and provides clear evidence of local moments. A second contribution proportional to the number of α-decays grows more slowly, showing indications of non-Fermi liquid behavior. This contribution can be fit to a $-ln$(T) temperature dependence for both allotropes suggesting a disordered Kondo model, while the α-Pu phase is also a candidate for the quantum Griffiths phase model. Both models arise from disorder driven interactions coupling local moments with the conduction electrons, suggesting a complex interplay between the defects and electronic properties that provide insight into the fundamental nature of plutonium. In the PuAm alloy near 25% Am concentration, a low temperature damage induced phase transition arises which demonstrates a remarkably large magnetic moment that may be further evidence of proximity to a quantum critical point.

Acknowledgement

[1] S. McCall, M. J. Fluss, B. W. Chung, M. W. McElfresh, G. F. Chapline, and D. J. Jackson, *Materials Science Transactions* **8**, 35 (2005)..

[2] S. K. McCall, M. J. Fluss, B. W. Chung, M. W. McElfresh, G. F. Chapline, and D. D. Jackson, *J. Alloys Compd.* **444-445**, 168 (2007)..

[3] S. K. McCall, M. J. Fluss, B. W. Chung, M. W. McElfresh, D. D. Jackson, and G. F. Chapline, *PNAS* **103**, 17179 (2006)..

[4] R. H. Heffner, G. D. Morris, M. J. Fluss, B. Chung, S. McCall, D. E. MacLaughlin, L. Shu, K. Ohishi, E. D. Bauer, J. L. Sarrao, W. Higemoto, and T. U. Ito, *Phys. Rev. B* **73**, 094453 (2006)..

[5] R. H. Heffner, K. Ohishi, M. J. Fluss, G. D. Morris, D. E. MacLaughlin, L. Shu, B. W. Chung, S. K. McCall, E. D. Bauer, J. L. Sarrao, T. U. Ito, and W. Higemoto, *J. Alloys Compd.* **444-445**, 80 (2007)..

[6] G. Chapline, M. Fluss, and S. McCall, *J. Alloys Compd.* **444-445**, 142 (2007)..

[7] S. K. McCall, M. J. Fluss, B. W. Chung, M. W. McElfresh, and R. G. Haire, in Materials Research Society Fall Meeting 2006, edited by K. J. M. Blobaum (Boston MA, 2007), p. 0986..

[8] R. H. Heffner, G. D. Morris, M. J. Fluss, B. Chung, D. E. MacLaughlin, L. Shu, and J. E. Anderson,

Physica B: Condensed Matter **374-375**, 163 (2006)..

[9] P. Soderlind, and B. Sadigh, *Phys. Rev. Lett.* **92**, 185702 (2004)..

[10] P. Soderlind, A. Landa, and B. Sadigh, *Phys. Rev. B* **66**, 205109 (2002)..

[11] S. Y. Savrasov, and G. Kotliar, *Phys. Rev. Lett.* **84**, 3670 (2000)..

[12] S. Y. Savrasov, G. Kotliar, and E. Abrahams, *Nature* **410**, 793 (2001)..

[13] J. Bouchet, B. Siberchicot, F. Jollet, and A. Pasturel, *J. Phys.: Condens. Matter* **12**, 1723 (2000)..

[14] A. O. Shorikov, A. V. Lukoyanov, M. A. Korotin, and V. I. Anisimov, *Phys. Rev. B* **72**, 024458 (2005)..

[15] A. B. Shick, V. Drchal, and L. Havela, *Europhys. Lett.* **69**, 588 (2005)..

[16] J. C. Lashley, A. Lawson, R. J. McQueeney, and G. H. Lander, *Phys. Rev. B* **72**, 054416 (2005)..

[17] J. C. Lashley, J. Singleton, A. Migliori, J. B. Betts, R. A. Fisher, J. L. Smith, and R. J. McQueeney, *Phys. Rev. Lett.* **91**, 205901/1 (2003)..

[18] A. M. Clogston, B. T. Matthias, M. Peter, H. J. Williams, E. Corenzwit, and R. C. Sherwood, *Physical Review* **125**, 541 (1962)..

[19] R. M. Bozorth, P. A. Wolff, D. D. Davis, V. B. Compton, and J. H. Wernick, *Physical Review* **122**, 1157 (1961)..

[20] H. H. Hill, J. D. G. Lindsay, R. W. White, L. B. Asprey, V. O. Struebing, and B. T. Matthias, *Physica* **55**, 615 (1971)..

[21] P. Mendels, J. Bobroff, G. Collin, H. Alloul, M. Gabay, J. F. Marucco, N. Blanchard, and B. Grenier, *Europhys. Lett.* **46**, 678 (1999)..

[22] J. Bobroff, W. A. MacFarlane, H. Alloul, P. Mendels, N. Blanchard, G. Collin, and J. F. Marucco, *Phys. Rev. Lett.* **83**, 4381 (1999)..

[23] F. Rullier-Albenque, H. Alloul, and R. Tourbot, *Phys. Rev. Lett.* **91**, 047001 (2003)..

[24] T. Diaz de la Rubia, M. J. Caturla, E. Alonso, M. J. Fluss, and J. M. Perlado, *Journal of Computer-Aided Materials Design* **5**, 243 (1998)..

[25] D. A. Wigley, *Proc. R. Soc. London, A* **284**, 344 (1965)..

[26] J. A. Lee, K. Mendelssohn, and D. A. Wigley, *Phys. Lett. A* **1**, 325 (1962)..

[27] M. J. Mortimer, J. A. C. Marples, and J. A. Lee, *Int. Met. Rev.* **20**, 109 (1975)..

[28] R. O. Elliott, C. E. Olsen, and G. H. Vineyard, *Acta Metal.* **11**, 1129 (1963)..

[29] M. J. Fluss, B. D. Wirth, M. Wall, T. E. Felter, M. J. Caturla, A. Kubota, and T. D. de la Rubia, *J. Alloys Compd.* **368**, 62 (2004)..

[30] J.-M. Fournier, and R. Troc, in *Handbook on the Physics and Chemistry of the Actinides*, edited by A. J. Freeman, and G. H. Lander (North-Holland, New York, 1985)..

[31] K. T. Moore, M. A. Wall, and A. J. Schwartz, *J. Nucl. Mater.* **306**, 213 (2002)..

[32] P. Boulet, E. Colineau, F. Wastin, P. Javorsky, J. C. Griveau, J. Rebizant, G. R. Stewart, and E. D. Bauer, *Phys. Rev. B* **72**, 64438 (2005)..

[33] P. Boulet, E. Colineau, P. Javorsky, F. Wastin, and J. Rebizant, *J. Alloys Compd.* **394**, 93 (2005)..

[34] S. Meot-Reymond, and J. M. Fournier, *J. Alloys Compd.* **232**, 119 (1996)..

[35] M. J. Fluss, in Plutonium Futures - the Science. Third Topical Conference on Plutonium and Actinides. Albuquerque, NM, edited 2003)..

[36] in *The definition of nearest neighbor is less clear in a low symmetry monoclinic structure that includes 8 inequivalent lattice sites. Using the less dense delta fcc interatomic distance as the limit for nearest neighbors results in 12 +/- 1 depending on the lattice site considered.* ..

[37] O. O. Bernal, D. E. MacLaughlin, H. G. Lukefahr, and B. Andraka, *Phys. Rev. Lett.* **75**, 2023 (1995)..

[38] E. Miranda, V. Dobrosavljevic, and G. Kotliar, *Phys. Rev. Lett.* **78**, 290 (1997)..

[39] E. Miranda, V. Dobrosavljevic, and G. Kotliar, *J. Phys.: Condens. Matter* **8**, 9871..

[40] A. H. C. Neto, G. Castilla, and B. A. Jones, *Phys. Rev. Lett.* **81**, 3531 (1998)..

[41] A. H. C. Neto, and B. A. Jones, *Phys. Rev. B* **62**, 14975 (2000)..

[42] R. B. Griffiths, *Phys. Rev. Lett.* **23**, 17 (1969)..

[43] A. Jagannathan, E. Abrahams, and M. J. Stephen, *Phys. Rev. B* **37**, 436 (1988)..

[44] A. Migliori, H. Ledbetter, A. C. Lawson, A. P. Ramirez, D. A. Miller, J. B. Betts, M. Ramos, and J. C. Lashley, *Phys. Rev. B* **73**, 052101 (2006)..

[45] M. Dormeval, Ph.D. thesis, Universite de Bourgogne, 2001.

[46] N. Baclet, M. Dormeval, P. P, J. M. Fournier, F. Wastin, E. Colineau, J. Rebizant, and G. H. Lander, *J. Nucl. Sci. Technol.* **Suppl. 3**, 148 (2002)..